BL23SU
JAEA Actinide Science II

1. Abstract

The JAEA actinide science beamline BL23SU is mainly dedicated to actinide material science. The beamline is also utilized for surface chemistry. There are two end-stations in the beamline: real-time photoelectron spectroscopy station in the experimental hall and actinide science stations in the RI Laboratory building.

2. Surface chemistry experimental end-station

The surface chemistry end-station in the experimental hall at BL23SU focuses on the chemical reactions and functionalities of surfaces/interfaces of solids. Soft X-ray photoelectron spectroscopy is used to conduct chemical analyses of surfaces. This station has been employed to promote the nanotechnology platform of the Ministry of Education, Culture, Sports, Science and Technology (MEXT) of Japan as a member of the advanced characterization nanotechnology platform to establish the shared use of advanced characterization equipment. The apparatus is widely used for research studies on physicochemical properties, functionalities of surface/interface of materials, and mechanisms of surface reactions.

The gas-barrier properties of graphene hold great interest from both scientific and technological perspectives. In situ photoelectron spectroscopy was used to demonstrate the gas-barrier performance of graphene for oxygen molecules having sub-electron volt kinetic energy, while it retains its gas-barrier performance for non-energetic molecules. It was also found that the permeation process is nondestructive. Molecular-dynamics-based simulation suggests kinetic-energy-mediated reactions catalyzed by common graphene defects as a responsible mechanism [1]. This work was described in a press release [2].

Nickel (Ni) is an important material as a catalyst for nitric oxide decomposition and ammonia production. The reduction processes of ultrathin oxide on Ni(111) surfaces in a hydrogen atmosphere were studied by in situ time-resolved photoelectron spectroscopy. A new reaction model showing that the reduction on heating under vacuum does not yield a clean Ni(111) surface was presented. Conversely, in a hydrogen atmosphere, the Ni oxide was completely reduced and a clean Ni(111) surface was obtained. The reduction was explained by a two-step reaction model: the rate-limiting process for the first step is the surface precipitation of oxygen atoms and that for the second step is the dissociation of H_2 molecules [3].

Ni-based alloys are widely used in chemical plants. In this study, the behaviors of Ni-Sn and Ni-Sb alloys under a high-temperature oxidation environment were studied by in situ photoelectron spectroscopy. It was confirmed that Sn and Sb were segregated at the surface during oxidation in low oxygen potential. This result showed that the segregation of Sn and Sb significantly improves the metal dusting resistance [4].

The oxidation of metal alloys is more complex than that of a pure metal because of the segregation of atoms and the formation of multiple oxides. Here, the oxidation of $Cu_3Pd(111)$ and $Cu_3Pt(111)$ using 2.3 eV oxygen was studied by in

situ photoelectron spectroscopy. It was found that CuO forms on both surfaces. When the surface temperature increases to 500 K, Cu_2O also forms on $Cu_3Pd(111)$, but not on $Cu_3Pt(111)$. For comparison, Cu_2O forms even at 300 K on Cu(111). On $Cu_3Au(111)$, Cu_2O forms only after 500 K, and no oxides were observed at 300 K. These results imply the mobility of interfacial species (Cu/Pd/Pt) and charge transfer between surface Cu oxides and subsurface species (Cu/Pd/Pt) [5]. This work was also described in a press release [6].

GaN is an attractive material for the application of power electronic devices. The initial O_2 adsorption behavior of different GaN surfaces (the polar Ga-face and N-face and the nonpolar $(10\bar{1}0)$) was studied by the combined use of real-time photoelectron spectroscopy and oxygen molecular beams. The theoretical results based on density functional molecular dynamics calculations describe the adsorption dynamics, adsorption sites, and oxide structure depending on surface planes. The computational model including both the surface spin and polarity of GaN is useful for understanding the interface between GaN and oxide layers in metal−oxide electronic devices [7].

As described above, studies on the reactions and chemical analysis of solid surfaces of various functional materials have been conducted at the surface chemistry experimental end-station.

3. Actinide science stations

In the RI Laboratory building, the photoelectron spectroscopy station and soft X-ray magnetic circular dichroism (MCD) stations are in operation . In addition, the commissioning of a newly developed scanning transmission X-ray microscopy (STXM) station has started.

In the photoelectron spectroscopy station, photoelectron spectroscopy studies for strongly correlated materials such as actinide and rare-earth compounds have been conducted. As a scientific result, the three-dimensional (3D) electronic structure of the hidden-order compound URu_2Si_2 was revealed using 3D angle-resolved photoelectron spectroscopy (ARPES), where the electronic structure of the entire Brillouin zone is obtained by scanning both the incident photon energy and detection angles of photoelectrons [8]. Figure 1 shows the experimental ARPES spectra of URu_2Si_2 within k_x-k_y and $k_{//}$-k_z planes. The quasi-particle bands with enhanced contribution from the U 5*f* state were observed near E_F, formed by the hybridization with the Ru 4*d* states. The energy dispersion of the quasi-particle band significantly depends on k_z, indicating that they inherently have a 3D nature. The band-structure calculation qualitatively explains the characteristic features of the band structure and Fermi surface, although the electron correlation effect strongly renormalizes the quasi-particle bands. We found that the 3D and strongly correlated nature of the quasi-particle bands in URu_2Si_2 is an essential ingredient for modeling its hidden-order transition. The ARPES experiments for the heavy fermion superconductor UTe_2 [9,10] and Eu-based compounds [12,13] were also conducted.

In the first half of FY2020, most of the experiments using the soft X-ray magnetic circular dichroism (XMCD) in the RI Laboratory were cancelled owing to the COVID-19 pandemic. From the second half of FY2020, the experiments have been conducted as usual. At the XMCD experimental station, we have promoted a wide

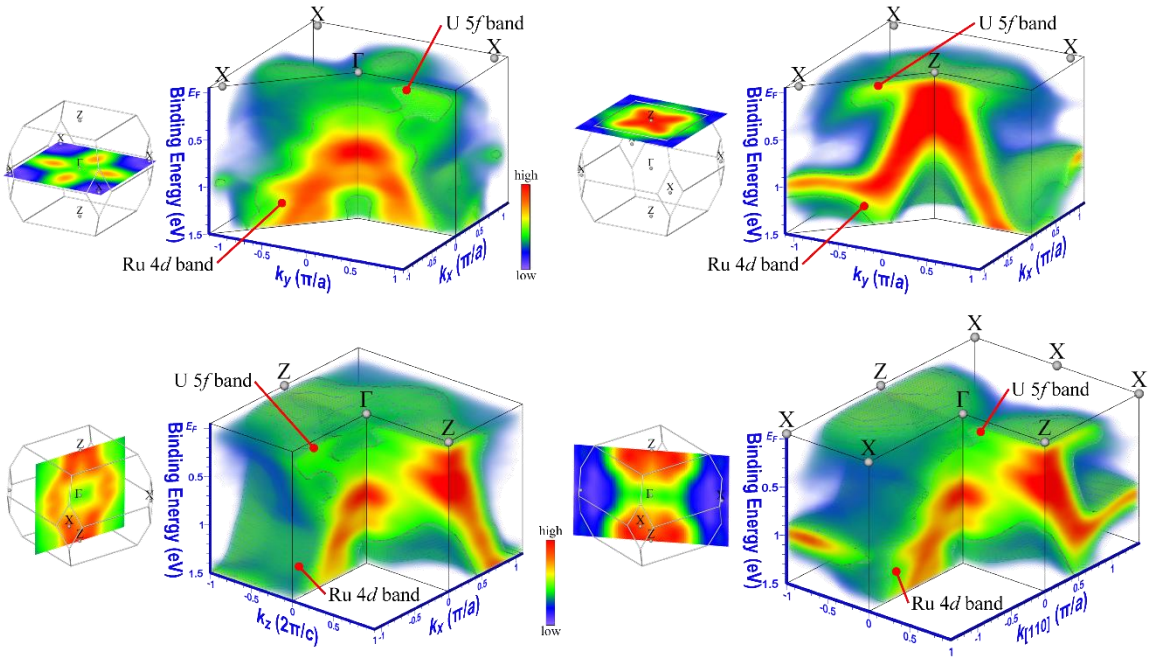

Fig. 1. Experimental ARPES spectra of URu_2Si_2 within k_x-k_y and $k_{//}$-k_z planes

range of research on strongly correlated electrons systems such as the 4*f* and 5*f* compounds, as well as topological insulators and functional magnetic materials [14–21]. Among them, two research results were released to the press. One is about the fabrication of a novel magnetic topological heterostructure, $Mn_4Bi_2Te_7/Bi_2Te_3$, where multiple magnetic layers are inserted into the topmost quintuple layer of the original topological insulator Bi_2Te_3. The relationship between a Dirac cone gap and the magnetic properties of the Mn 3*d* electrons has been revealed using XMCD. Hirahara et al. succeeded in observing that the gap in the surface state exists up to a temperature one order of magnitude higher than the temperature at which the magnetic order disappears, and eventually closes [17]. The other is about a ferromagnetic semiconductor. The magnetic ordering process of the Mn 3*d* electrons in $Ga_{1-x}Mn_xAs$ has been clarified through temperature- and magnetic-field-dependent XMCD experiments [19]. This result was selected as a featured paper and the cover of the issue, and an explanatory article was also published. In microscopic magnetic investigations for new and novel materials such as topological insulators and ferromagnetic semiconductors, XMCD has increasingly become an indispensable experimental tool in recent years.

Akitaka Yoshigoe, Yukiharu Takeda, and Shin-ichi Fujimori

Japan Atomic Energy Agency, Materials Sciences Research Center

References:

[1] Ogawa, S. et al. (2020). *J. Phys. Chem. Lett.* **11**, 9159.

[2] http://www.spring8.or.jp/ja/news_publications/press_release/2020/201026/

[3] Ogawa, S. et al. (2020). *J. Vac. Sci. Technol., A* **39**, 043207.

[4] Doi, T. et al. (2020). *Surf. Interface Anal.* **52**,

1117.

[5] Tsuda, T. et al. (2021). *Sci. Rep*. **11**, 3906.

[6] http://www.spring8.or.jp/ja/news_publications/press_release/2021/210219_2/

[7] Sumiya, M. et al. (2020). *J. Phys. Chem. C*. **124**, 25282.

[8] Fujimori, S. et al. (2021). *Electron. Struct.* **3**, 024008.

[9] Shick, A. B. Fujimori S. & Pickett, W. E. (2021). *Phys. Rev. B* **103**, 12513.

[10] Fujimori, S. et al. (2021). *J. Phys. Soc. Jpn.* **90**, 015002.

[11] Kataoka, N. et al. (2021). *J. Phys.: Cond. Mater.* **33**, 035501.

[12] Usachov, D. U. et al. (2020). *Phys. Rev. B* **102**, 205102.

[13] Kawasaki, I. et al. (2020). *J. Phys. Soc. Jpn.* **89**, 044704.

[14] Takeda, T. et al. (2020). *Phys. Rev. B* **101**, 155142.

[15] Yoshikawa, T. et al. (2020). *Phys. Rev. B* **102**, 064428.

[16] Saitoh, Y. et al. (2020). *Phys. Rev. B* **102**, 165152.

[17] Hirahara, T. et al. (2020). *Nat. Commun*. **11**, 4821.

[18] Fujisawa, Y. et al. (2020). *Phys. Rev. Mater*. **4**, 114001.

[19] Takeda, Y. et al. (2020). *J. Appl. Phys*. **128**, 213902.

[20] Takeda, T. et al. (2020). *Phys. Rev. B* **102**, 245203.

[21] Ieda, J. et al. (2021). *Nano Lett.* **21**, 1807.